KfK 3580
September 1983

Calculated Efficiency of a 4 π Detector of BGO or BaF_2 for Monoenergetic Gamma Rays and Gamma Cascades Following Neutron Capture

K. Wisshak, F. Käppeler, G. Schatz
Institut für Kernphysik

Kernforschungszentrum Karlsruhe

KERNFORSCHUNGSZENTRUM KARLSRUHE
Institut für Kernphysik

KfK 3580

Calculated Efficiency of a 4π Detector of BGO or BaF_2 for Monoenergetic Gamma Rays and Gamma Cascades Following Neutron Capture

K. Wisshak, F. Käppeler, and G. Schatz

Kernforschungszentrum Karlsruhe GmbH, Karlsruhe

Kernforschungszentrum Karlsruhe GmbH
ISSN 0303-4003

ABSTRACT

The applicability of a spherical shell of BGO or BaF_2 as a 4π detector for high precision measurements of neutron capture cross sections was investigated. First the efficiency of both scintillator materials for monoenergetic gamma rays was calculated in the energy range from 0.5 to 10 MeV. Configurations with different thicknesses and inner radii were considered. Second, neutron capture cascades were calculated for several isotopes with widely different capture gamma ray spectra according to the statistical model. Both informations together allowed to determine the efficiency of an actual detector for neutron capture events in dependence of the threshold energy. A thickness of 10 cm BGO or 17.5 cm BaF_2 proved to be sufficient to registrate more than 95 % of all capture events above a threshold energy of 3 MeV. This reduces the systematic uncertainty due to the detector efficiency in an absolute cross section measurement to less than 1 % and in a relative measurement using a gold standard to less than 0.5 %.

ZUSAMMENFASSUNG

Berechnung der Ansprechwahrscheinlichkeit eines 4π Detektors aus BGO oder BaF_2 für monoenergetische Gammastrahlung und Gamma Kaskaden nach Neutroneneinfang.

Es wurde untersucht, ob ein 4π Detektor aus BGO oder BaF_2 für sehr genaue Messungen von Neutroneneinfangquerschnitten geeignet ist. Dazu wurde die Ansprechwahrscheinlichkeit beider Szintillatoren für monoenergetische Gammastrahlung im Energiebereich von 0.5 bis 10 MeV berechnet. Als zweites wurden Gamma Kaskaden, die bei Neutroneneinfang emittiert werden, für verschiedene Isotope mit sehr unterschiedlichen Einfangspektren nach dem statistischen Modell berechnet. Beide Informationen zusammen erlauben es, die Ansprechwahrscheinlichkeit eines Detektors für Neutroneneinfang in Abhängigkeit von der Nachweisschwelle zu bestimmen. Eine Dicke von 10 cm BGO oder 17.5 cm BaF_2 ist ausreichend, um mehr als 95 % aller Einfangereignisse oberhalb einer Schwelle von 3 MeV nachzuweisen. Dadurch wird der systematische Fehler, der durch die Nachweiswahrscheinlichkeit des Detektors bedingt ist, auf weniger als 1 % in einer Absolutmessung und auf weniger als 0.5 % in einer Relativmessung mit Gold als Standardquerschnitt reduziert.

I. INTRODUCTION

Recently a proposal has been made [1] to built a 4π detector for high precision measurements of neutron capture cross sections in the keV range. The justification of such an instrument can be found mainly in two fields (i) In nuclear astrophysics the investigation of nucleosynthesis requires detailed knowledge of nuclear reaction rates. Especially, the production of heavy elements in the so called s-process (slow neutron capture process) calls for very accurate measurements of neutron capture cross sections [1]. If a precision of 0.5 - 1 % can be reached it will be possible to determine the s-process age as well as its physical conditions as temperature, neutron density etc. The answer to these questions has a general impact on models of stellar and galactic evolution. (ii) Many requests still exist in connection with reactor design, fuel reprocessing and storage. There, an accuracy up to $\sim$ 1 % is needed for the most important cross sections like neutron capture in ^{238}U.

The present experimental techniques for neutron capture measurements are restricted to an accuracy of $\sim$ 4 - 5 % (Ref. 1) which is not sufficient to meet the requirements formulated above. It was therefore proposed to use instead a 4π detector with good energy resolution and near 100 % efficiency for gamma-ray energies up to 10 MeV.

This idea can be realized using bismuth germanate as detector material. Scintillation crystals of bismuth germanate, $Bi_4Ge_3O_{12}$ (BGO) are of rapidly increasing importance as gamma detectors in nuclear physics [2,3] or as shower detectors in particle physics [4,5]. With the availability of large size crystals numerous proposals have been made for 4π detector systems [6,7,8] in order to measure as completely as possible the energy and angular distribution of gamma cascades populated in (HI,xn) reactions. BGO offers the advantage of a very high density (ρ = 7.13 gcm^{-3}). This allows to reduce the active volume by a factor of $\sim$ 10 compared to a NaI detector with equal efficiency, resulting in a less compli-

cated set-up and compensating for the higher price of BGO. Even more important, it also ensures a significantly lower sensitivity for capture of slow neutrons which are the main source of background in this type of experiments. The main disadvantage is the low light output of BGO which restricts energy and time resolution to values which are a factor of 2 - 3 lower than for NaI. As in measurements of neutron capture cross sections the neutron energy is determined by the time of flight (TOF) technique, the energy resolution is restricted. This can be compensated only by an increase of the flight path which causes a strong reduction of the neutron flux at the sample position.

In this respect BaF_2 offers ideal conditions as the fast ultraviolet component in light emission at 220 nm allows for a subnanosecond timing [9]. The density of BaF_2 is 4.88 g/cm³ and thus its specific efficiency is between that of NaI and BGO. The small neutron capture cross section of barium restricts the sensitivity to low energetic neutrons to about the same level as for BGO even if one takes into account that a detector with the same efficiency has a much larger volume. A further advantage is the low price of BaF_2 crystals which are widely used as windows in UV-spectroscopy.

The aim of the present paper is to evaluate the optimum thickness of a spherical shell of BGO and BaF_2 with respect to the following requirements:

1.) The systematic uncertainty caused by the detector efficiency should be less than 1 % in an absolute measurement of neutron capture cross sections.

2.) The systematic uncertainty caused by the detector efficiency should be less than 0.5 % in a relative measurement of the ratio of two neutron capture cross sections.

3.) Capture events should be detected only above a threshold energy of 2 - 3 MeV, which is necessary to suppress low energy background.

4.) The inner radius of the shell should be 8 - 10 cm, to allow for time of flight discrimination of scattered neutrons (see Ref. 1).

5.) The detector should be composed of as few individual parts as possible to avoid efficiency losses at the borders and to allow for optimum light collection (32 - 42 elements).

6.) The individual detector element should be machined from a cylindrycal crystal not larger than 10 cm in diameter in case of BGO and 15 cm diameter in case of BaF_2, which seem to be the maximum size presently available.

Our calculations were carried out in four steps:

1.) The efficiency of a spherical shell of the respective scintillator material, (inner radius R_i and outher radius R_o) to monoenergetic gamma-rays in the energy range from 0 to 10 MeV was calculated analytically.

2. Capture cascades of several isotopes with widely differing binding energies and level densities were calculated in the framework of the statistical model.

3.) The efficiency for a single capture cascade was evaluated as a function of the threshold energy. Finally, the overall efficiency was determined by weighting the results for the individual cascades with their respective probability.

4.) The results obtained for a fixed threshold energy but with different assumptions for the geometry (step 1) and with widely different capture gamma-ray spectra (step 2) led to a realistic estimate of the systematic uncertainty caused by the detector efficiency in an actual measurement.

We do not discuss here the sensitivity of such a detector to scattered neutrons which may be another important source of uncertainty and give only some qualitative arguments at the end of the paper. This problem has already been discussed in Ref. 1 and will be covered on a more quantitative basis in future calculations.

II. CALCULATION OF THE EFFICIENCY FOR MONOENERGETIC GAMMA-RAYS

The efficiency of a spherical shell of BGO and BaF_2 to monoenergetic gamma-rays was calculated analytically considering up to three subsequent interactions. This code is described in detail in Ref. 10 and therefore we restrict ourselves to enumerate the individual processes considered:

P(O): Probability that no interaction occurs
P(C): Probability for Compton scattering
P(F): Probability for photo absorption
P(P): Probability for pair production

These interactions are composed of the following parts:

P(C) =	P(CO)	Compton scattering without interaction of the scattered gamma-ray.
	+P(CC)	Twofold Compton scattering
	+P(CF)	Compton scattering followed by photoabsorption of the scattered gamma-ray
	+P(CP)	Compton scattering and pair production of the scattered gamma-ray
P(P) =	P(P2F)	Pair production and photoabsorption of both annihilation quanta
	+P(P2C)	Pair production and Compton scattering of both annihilation quanta
	+P(PFC)	Pair production and photoabsorption of one, Compton scattering of the other annihilation quantum
	+P(PEF)	Pair production and photoabsorption of one annihilation quantum while the other escapes
	+P(PEC)	Pair production and Compton scattering of one annihilation quantum while the other escapes.

Finally, P(CC) is the sum of the following interactions:

P(CC) =	P(CCO)	Escape of the gamma-ray remaining after twofold Compton scattering
	+P(CCF)	Photoabsorption of the gamma-ray remaining after twofold Compton scattering
	+P(CCC)	Threefold Compton scattering
	+P(CCP)	Pair production after twofold Compton scattering.

The probability that the total energy of the gamma-ray is absorbed in the scintillator is given by:

$$P(FTOT) = P(F) + P(CF) + P(P2F) + P(CCF)$$

The efficiency for monoenergetic gamma-rays was calculated in steps of 1 MeV up to 10 MeV. The thickness of the spherical shell was chosen between 8 cm and 12 cm for BGO and between 12.5 cm and 20 cm for BaF_2 with R_i and R_o as compiled in Table I. These dimensions are a compromise between detector volume and an optimal time-of-flight discrimination of scattered neutrons (Ref. 1).

The code calculates the probability SW to detect a gamma-ray with energy E_γ above a threshold energy E_s. Simplifying assumptions were made for some of the interactions which are described in detail in Ref. 10. In order to avoid biasing, these assumptions were made in an optimistic and a pessimistic way with respect to the efficiency. Consequently, the results are given as SW(MAX) and SW(MIN) which represent an upper and lower limit for the true detection probability.

As an example we have compiled in Table II all interactions considered for the BGO configuration I (R_i = 10 cm, R_o = 20 cm). This is to demonstrate the relative size of the individual components and to show that the approximations assumed for e.g. P(CP), and P(CCP) (see Ref. 10) affect quantities which are generally small. The second column gives the probability that no energy is released in the crystal. It reflects the minimum of the total attenuation coefficient of BGO around $\sim$ 5 MeV where this probability is $\sim$ 6 %. The last column gives the probability to detect

the total gamma energy. It drops very rapidly to ∿ 30 % at higher energies which at a first glance seems to be very low. One has to keep in mind, however, that in many interaction processes not all but almost all energy is released in the detector. If, therefore, the energy resolution of ∿ 10 % of BGO is considered, a much higher percentage of events falls in the full energy peak of an actual spectrum.

In Table III the output of the code for SW(MAX) and SW(MIN) is given for one energy point of the above example at 5 MeV. It can be seen that the difference is negligible at low energies and only significant in the very upper end of the spectrum (above ∿ 4 MeV). The assumptions of SW(MAX) shift a large fraction of events from lower energies into the full energy peak.

The gamma spectrum recorded by a detector is given by the derivative of SW folded with the respective energy resolution. To simulate this we assumed a constant resolution of ∿ 10 % and divided each gamma energy E_γ in ten equal parts. The gamma intensity is then given by the difference in SW between the lower and upper energy of the respective bin. The results for six BGO and four BaF_2 configurations (see Table I) are summarized in Tables IV to XIII. As an example, Fig. 1 shows the spectra for monoenergetic gamma-rays calculated for the BGO configuration I (R_i = 10 cm, R_o = 20 cm) with the conservative lower limit for the detection probability, SW(MIN). The full energy peak contains 60 - 90 % of the efficiency for energies between 2 MeV and 10 MeV. In cases were the peak efficiency is low most of the remaining intensity is found in the neighboring bins. The first bin is dominated by the probability that the gamma-ray escapes without interaction. The respective probability is ∿ 6 % for this configuration. The intensity in the intermediate bins 2 to 6 is generally below 1 %.

As can be seen from Table VI the full energy peak (always assuming SW(MIN)) increases to 70 - 95 % for energies between 2 and 10 MeV if the thickness of the BGO crystal shell is increased from 10 to 12 cm. In that case only 3-4 % of the gamma-rays escape without interaction. Reducing the thickness to 8 cm decreases

the peak efficiency to 50 - 85 % while the losses are increasing to 9 - 11 %. Generally, the differences between configurations of equal thickness but different radii are small. A comparison of Tables IV and XII shows that 10 cm of BGO have about the same efficiency as 17.5 cm of BaF_2.

III. EFFICIENCY FOR GAMMA CASCADES FOLLOWING NEUTRON CAPTURE

To calculate the efficiency of a spherical shell of BGO or BaF_2 for neutron capture events we chose three examples which represent typical capture gamma-ray spectra: capture in ^{241}Am, ^{197}Au and ^{56}Fe. The high level density in the ^{242}Am compound nucleus leads to capture cascades with a high gamma-ray multiplicity and consequently to a soft gamma-ray spectrum. Contrary, the low level density in ^{57}Fe yields a low multiplicity and therefore the spectrum is dominated by a hard component from direct transitions to the groundstate. Neutron capture in gold can be regarded as an intermediate case. For these three isotopes individual capture cascades have been calculated in the framework of the statistical model as described in detail in Refs.11,12 and 13.

In these calculations which were performed for a neutron energy of 30 keV up to $\sim$ 20000 cascades were determined for each isotope, together with the respective partial cross sections. For the purpose of the present efficiency calculations we selected the cascades with the highest partial cross section. As shown in Table XIV the binding energy and consequently the energy of the capture cascade varies between 5.6 and 7.7 MeV for the three examples. The average multiplicity of the capture cascades changes between 3 and 5. A total number of 1000 cascades was sufficient to cover more than 75 % of the total capture cross section in case of ^{241}Am and ^{197}Au while for ^{56}Fe only 300 cascades accounted for more than 96 %.

For completeness Table XV lists for each isotope the ten cascades with the highest partial cross sections and illustrates the above arguments. In case of ^{241}Am eight cascades with multiplicity 4 are observed each covering a partial cross section of less than 1 % only. Contrary, in ^{56}Fe the first two cascades which lead directly to the ground state or the first excited state cover already $\sim$ 20 % of the total capture cross section. Fig. 2 demonstrates that the total capture gamma-ray spectra for all isotopes are significantly different in shape.

The energy spectrum which will be measured using a spherical shell of BGO or BaF_2 for a fixed capture cascade emitted from the center, was calculated in the following way: the energy of each gamma-ray in the cascade with multiplicity K was divided into ten equal energy bins, E_i (i = 1...10) according to the representation in Fig. 1. The detection probability of each bin, $P(E_i)$ was obtained by a linear interpolation between the respective values for neighboring monoenergetic gamma-rays (Tables IV to XIII). The energy spectrum for a particular cascade was then obtained by combining the detection probabilities for the individual gamma-rays considering all possible combinations of all energy bins:

$$P(E_\Sigma) = \prod_{i,j\ldots x=1}^{10} P_1(E_i)\cdot P_2(E_j)\ldots P_K(E_x)$$

where the index 1,2...K enumerates the various cascade gamma-rays, K being the multiplicity. For each combination, the detected gamma-ray energy is the sum of the respective bin energies:

$$E_\Sigma = E_i + E_j + \ldots + E_x \quad (i,j\ldots x=1\ldots 10)$$

All these pairs $P(E_\Sigma)$, E_Σ are then sorted to give the final energy spectrum of the cascade.

Finally, the results for the individual cascades were summed up and weighted with the corresponding partial capture cross section in order to get the spectrum which can be expected in an actual measurement.

In Tables XVI to XXI the final results of the efficiency of a spherical shell of BGO or BaF_2 for capture in ^{241}Am, ^{197}Au and ^{56}Fe are compiled. The results obtained for the optimistic and pessimistic view of the detection probability for monoenergetic gamma-rays are quoted separately. The numbers given are the probabilities in % to detect a capture event above the threshold energy E_s. The pulse height spectra as expected for a spherical shell of BGO with 10 cm thickness and R_i = 10, R_o = 20 cm are plotted in Fig. 3. It has to be noted, that the resolution of the full energy peak is mainly determined by the number of gamma-rays escaping from the crystal and not by the energy resolution. It depends therefore on the thickness of the detector and deteriorates rapidly if this falls below 10 cm.

It was mentioned above that an electronic threshold has to be set in an actual measurement of capture events in order to suppress low energy background. Fig. 4 shows a background spectrum taken with a cylindrical 10 cm x 10 cm BGO detector in a measuring time of 24 h. The background is dominated by the gamma-ray lines from the decay of ^{40}K (1.4 MeV) and from the decay of ^{212}Po and ^{208}Tl. (2.6 MeV) At higher energies the background drops by two orders of magnitude. This suggests to choose a threshold energy around 3 MeV. In that case the following conclusions can be drawn from Tables XVI to XXI:

1.) The differences in efficiency between SW(MIN) and SW(MAX) is on the average 0.4 %, 0.7 % and 1.2 % for BGO crystals with 12 cm, 10 cm and 8 cm thickness, respectively. The corresponding values range between 0.7 % and 1.9 % for BaF_2 crystals with thicknesses between 20 cm and 12.5 cm. This indicates that the systematic uncertainty in the efficiency calculation due to the approximations in the code is less than 0.5 % if a thickness of at least 10 cm BGO or 17 cm BaF_2 is chosen.

2.) The absolute detection efficiency is $\sim$ 95 % for a 10 cm thick BGO detector. It increases to 97 % for 12 cm, but decreases to 91 % for 8 cm thickness. A BaF_2 detector of 17.5 cm thickness is compatible to a BGO crystall of 10 cm thickness.

3.) The difference in efficiency for neutron capture cascades from nuclei with widely different binding energies, gamma-ray multiplicities and capture gamma-ray spectra is ∿ 1 % for a 10 cm thick BGO detector. It decreases to 0.5 % for 12 cm and increases to 1.5 % for 8 cm thickness. Thus the systematic uncertainty caused by the calculation of capture cascades is certainly less than 0.3 % if a thickness of at least 10 cm is chosen.

4.) The efficiency is very insensitive to a change of the inner radius by 2 cm.

From the above points one may conclude that the absolute efficiency can be determined with an accuracy of better than 1 %. However, a spherical shell of at least 10 cm BGO or 17 cm BaF_2 thickness should be used for the final design.

In absolute measurements of capture cross sections the neutron flux has to be determined with the same accuracy as the capture rate. As this may be problematic in most applications, relative measurements are preferable. In these cases many systematic uncertainties like e.g. gamma-ray self-absorption in the sample or multiple scattering are strongly reduced or cancel out, and the flux determination is avoided. Especially in investigations for nuclear astrophysics most of the interesting questions can be solved by very accurate measurements of cross section ratios (Ref. 1).

With gold as a standard we illustrate the situation at the example of a relative measurement $\sigma_\gamma(^{56}Fe)/\sigma_\gamma(^{197}Au)$ and $\sigma_\gamma(^{241}Am)/\sigma_\gamma(^{197}Au)$. In Tables XXII and XXIII the difference of the efficiency for sample and reference sample is given as a function of the threshold energy E_s for all configurations considered here. It is found that this difference is of the order of 1 % or even less if a BGO detector thickness of a least 10 cm or a BaF_2 detector thickness of 17 cm is chosen. The results differ in general by less than 0.5 % between the two assumptions SW(MIN) and SW(MAX). Keeping in mind that the present examples represent cases with extreme differences in the capture

gamma-ray spectra, binding energies and cascade multiplicities one may conclude that the systematic uncertainty in a relative measurement due to the difference in efficiency can be reduced to less than 0.5 % for most practical applications. This holds especially for the suggested measurements in nuclear astrophysics (Ref. 1) where cross section ratios of neighboring nuclei have to be determined.

CONCLUSIONS

A spherical shell of BGO with $\sim$ 10 cm thickness or BaF_2 with $\sim$ 17 cm thickness and an inner radius of 8 - 10 cm offers an efficiency for gamma-ray cascades following neutron capture which is high enough to reduce the correlated systematic uncertainty to less than 1 % in absolute measurements and less than 0.5 % in relative measurements. This holds even for isotopes with widely different binding energies, capture gamma-ray spectra and cascade multiplicities. It holds the more in case of an actual detector because then the theoretical calculation of the detection probability SW and the capture gamma-ray spectra can be replaced by direct measurements. Such a detector which can be realised with presently available crystals by subdivision into 32 or 42 elements (Ref. 1) will be able to increase the accuracy of present day techniques for capture cross section measurements at least by a factor of five. It will be able to meet the accuracy of nuclear data requirements for nuclear astrophysics as well as for reactor design.

The present paper concentrates on the detector efficiency but as the aspect of neutron sensitivity is also very important, we finally add some qualitative arguments showing that this will not severely affect the accuracy of the measurements.

1.) At low energies (in the eV range) neutrons scattered from the sample may be shielded effectively by a thin layer of ^{6}Li or ^{10}B inside the spherical shell.

2.) At higher energies (10 - 100 keV) time-of-flight discrimination of scattered neutrons is applicable if primary flight paths of 50-100 cm are used as it is possible at Van de Graaff accelerators. Moreover, in the keV range the ratio of scattering to capture in both scintillator materials is of the order of 20 - 100; therefore scattered neutrons have a high probability to escape from the detector before being captured because the scattering length is of the order of 2 cm. But if neutrons are captured after 5 - 10 scattering events the respective gamma-rays are also already delayed in time and can thus be discriminated from primary events.

These arguments, however, will be put on a more quantitative basis in a forthcoming publication.

ACKNOWLEDGMENTS

We would like to thank F. Fabbri and G. Reffo for making available the individual capture cascades needed for the present calculations. We appreciate very much the help of J. Oehlschläger in handling the code to calculate the efficiency for monoenergetic gamma-rays.

REFERENCES

1.) F. KÄPPELER, G. SCHATZ, and K. WISSHAK, "Vorschlag: ein 4π Wismuth-Germanat-Detektor für Präzisionsmessungen zur Elementsynthese im s-Prozess", KfK 3472, Kernforschungszentrum Karlsruhe 1983

2.) M. MOSZYNSKI, C. GRESSET, J. VACHER, and R. ODRU, Nucl. Instrum. Methods 188 (1981) 403

3.) D.M. DRAKE, L.R. NILSSON, and J. FAUCETT Nucl. Instrum. Methods 188 (1981) 313

4.) M. KOBAYASHI, S.I. KUROKAWA, S. SUGIMOTO, Y.YOSHIMURA, M. CHIBA, H. YOSHIDA, M. ISHII, S. AKIYAMA, and H. ISHIBASHI, Nucl. Instrum. Methods 189 (1981) 629

5.) P. PAVLOPOULOS, M. HASINOFF, J. REPOND, L. TAUSCHER, D. TRÖSTER, M. ROUSSEAU, K. FRANSSON, T. ALBERIS, and K. ZIOUTAS, Nucl. Instrum. Methods 197 (1982)331

6.) R.M. DIAMOND and F.S. STEPHENS, Proposal unpublished

7.) M.A. LONE, O. HÄUSSER, T.K. ALEXANDER, J. GASCON, E. HAGEBERG, Talk presented at the BGO Conference Princeton (1982)and private communications

8.) J.X. SALADIN, C. BAKTASH, I.Y. LEE, R. BLUE, R. RONNINGEN, and R.A. SORENSEN, Progress Report 1982 Michigan State University

9.) M.LAVAL, M. MOSZYNSKI, R. ALLEMAND, E.CORMORECHE, P.GUINET, R. ORDU, and J. VACHER, Nucl. Instrum. Methods 206 (1983) 169

10.) G. SCHATZ and J. OEHLSCHLÄGER KfK report to be published

11.) G. REFFO, F. FABBRI, K. WISSHAK, and F. KÄPPELER, Nucl. Sci. Eng. 80 (1982) 630

12.) K. WISSHAK, J. WICKENHAUSER, F. KÄPPELER, G. REFFO, and F. FABBRI, Nucl. Sci. Eng 81(1982) 396

13.) K. WISSHAK, F. KÄPPELER, G. REFFO, and F. FABBRI, "Neutron Capture in s-Wave Resonances of ^{56}Fe, ^{58}Ni, and ^{60}Ni", KfK 3515, Kernforschungszentrum Karlsruhe 1983

Table I. Different Geometrical Configurations of a Spherical Shell Used in the Present Efficiency Calculations

BGO

Configuration	R_i(cm)	R_o(cm)	d(cm)
I	10	20	10
II	8	18	10
III	9	21	12
IV	8	20	12
V	10	18	8
VI	8	16	8

BaF_2

Configuration	R_i(cm)	R_o(cm)	d(cm)
I	10	22.5	12.5
II	10	25	15
III	10	27.5	17.5
IV	10	30	20

Table II. Total Amount of the Individual Interaction Processes Considered in the Calculations, Configuration I, R_i=10cm, R_o=20cm.

(the numbers given in brackets is the respective exponent)

					P(C)				
E	P(0)	P(C)	P(F)	P(P)	P(CO)	P(CC)	P(CF)	P(CP)	P(P2F)
0.5	7.7(-5)	5.5(-1)	4.5(-1)	0.0	6.5(-5)	1.9(-1)	3.7(-1)	0.0	0.0
1.0	8.7(-3)	8.0(-1)	1.9(-1)	0.0	8.7(-3)	4.2(-1)	3.7(-1)	0.0	0.0
2.0	4.2(-2)	8.0(-1)	7.8(-2)	8.0(-2)	3.9(-2)	4.9(-1)	2.6(-1)	8.8(-3)	1.6(-2)
3.0	5.7(-2)	6.9(-1)	4.5(-2)	2.1(-1)	4.8(-2)	4.2(-1)	1.9(-1)	2.6(-2)	4.1(-2)
4.0	6.3(-2)	5.9(-1)	3.0(-2)	3.2(-1)	4.8(-2)	3.6(-1)	1.5(-1)	3.9(-2)	6.2(-2)
5.0	6.4(-2)	5.1(-1)	2.2(-2)	4.0(-1)	4.5(-2)	3.0(-1)	1.2(-1)	4.7(-2)	7.8(-2)
6.0	6.2(-2)	4.5(-1)	1.7(-2)	4.7(-1)	4.1(-2)	2.6(-1)	9.7(-2)	5.1(-2)	9.2(-2)
7.0	6.0(-2)	4.0(-1)	1.4(-2)	5.3(-1)	3.7(-2)	2.2(-1)	8.2(-2)	5.3(-2)	1.0(-1)
8.0	5.7(-2)	3.6(-1)	1.1(-2)	5.7(-1)	3.4(-2)	2.0(-1)	7.1(-2)	5.4(-2)	1.1(-1)
9.0	5.4(-2)	3.2(-1)	9.7(-3)	6.1(-1)	3.1(-2)	1.8(-1)	6.2(-2)	5.4(-2)	1.2(-1)
10.0	5.1(-2)	2.9(-1)	8.3(-3)	6.5(-1)	2.8(-2)	1.6(-1)	5.5(-2)	5.3(-2)	1.3(-1)

		P(P)				P(CC)			
E	P(P2C)	P(PFC)	P(PEF)	P(PEC)	P(CCO)	P(CCF)	P(CCC)	P(CCP)	PFTOT
0.5	0.0	0.0	0.0	0.0	9.0(-6)	1.4(-1)	4.4(-2)	0.0	9.6(-1)
1.0	0.0	0.0	0.0	0.0	5.1(-3)	2.5(-1)	1.7(-1)	0.0	8.1(-1)
2.0	2.5(-2)	3.9(-2)	3.8(-4)	4.8(-4)	4.0(-2)	2.2(-1)	2.3(-1)	9.4(-4)	5.8(-1)
3.0	6.4(-2)	1.0(-1)	1.2(-3)	1.5(-3)	5.1(-2)	1.7(-1)	2.0(-1)	3.4(-3)	4.5(-1)
4.0	9.7(-2)	1.6(-1)	1.9(-3)	2.4(-3)	5.0(-2)	1.4(-1)	1.7(-1)	5.1(-3)	3.7(-1)
5.0	1.2(-1)	2.0(-1)	2.5(-3)	3.1(-3)	4.4(-2)	1.1(-1)	1.4(-1)	5.9(-3)	3.3(-1)
6.0	1.4(-1)	2.3(-1)	2.8(-3)	3.6(-3)	3.8(-2)	9.4(-2)	1.2(-1)	6.2(-3)	3.0(-1)
7.0	1.6(-1)	2.6(-1)	3.1(-3)	3.9(-3)	3.3(-2)	7.9(-2)	1.1(-1)	6.3(-3)	2.8(-1)
8.0	1.8(-1)	2.8(-1)	3.3(-3)	4.1(-3)	2.8(-2)	7.0(-2)	9.4(-2)	6.1(-3)	2.6(-1)
9.0	1.9(-1)	3.0(-1)	3.4(-3)	4.3(-3)	2.4(-2)	6.3(-2)	8.3(-2)	5.9(-3)	2.5(-1)
10.0	2.0(-1)	3.2(-1)	3.4(-3)	4.3(-3)	2.1(-2)	5.7(-2)	7.5(-2)	5.6(-3)	2.5(-1)

Table III.Final Results for the Detection Probability SW in dependence of the Threshold energy E
(Configuration I, R_i=10cm, R_a=20cm, E_γ=5MeV)

E (MeV)	SW(MAX)	SW(MIN)
0.0	9.36350D-01	9.36350D-01
5.000D-02	9.35763D-01	9.35763D-01
1.000D-01	9.35177D-01	9.35177D-01
1.500D-01	9.34592D-01	9.34592D-01
2.000D-01	9.34008D-01	9.34008D-01
2.500D-01	9.33425D-01	9.33425D-01
3.000D-01	9.32843D-01	9.32842D-01
3.500D-01	9.32262D-01	9.32261D-01
4.000D-01	9.31682D-01	9.31680D-01
4.500D-01	9.31102D-01	9.31099D-01
5.000D-01	9.30524D-01	9.30519D-01
5.500D-01	9.29945D-01	9.29940D-01
6.000D-01	9.29368D-01	9.29360D-01
6.500D-01	9.28791D-01	9.28781D-01
7.000D-01	9.28214D-01	9.28202D-01
7.500D-01	9.27637D-01	9.27622D-01
8.000D-01	9.27061D-01	9.27042D-01
8.500D-01	9.26484D-01	9.26461D-01
9.000D-01	9.25908D-01	9.25880D-01
9.500D-01	9.25330D-01	9.25297D-01
1.000D+00	9.24753D-01	9.24713D-01
1.050D+00	9.24174D-01	9.24127D-01
1.100D+00	9.23594D-01	9.23540D-01
1.150D+00	9.23014D-01	9.22950D-01
1.200D+00	9.22432D-01	9.22358D-01
1.250D+00	9.21848D-01	9.21764D-01
1.300D+00	9.21264D-01	9.21167D-01
1.350D+00	9.20677D-01	9.20567D-01
1.400D+00	9.20089D-01	9.19963D-01
1.450D+00	9.19499D-01	9.19357D-01
1.500D+00	9.18908D-01	9.18747D-01
1.550D+00	9.18314D-01	9.18132D-01
1.600D+00	9.17717D-01	9.17514D-01
1.650D+00	9.17119D-01	9.16891D-01
1.700D+00	9.16518D-01	9.16263D-01
1.750D+00	9.15914D-01	9.15630D-01
1.800D+00	9.15308D-01	9.14991D-01
1.850D+00	9.14699D-01	9.14347D-01
1.900D+00	9.14086D-01	9.13697D-01
1.950D+00	9.13471D-01	9.13040D-01
2.000D+00	9.12852D-01	9.12376D-01
2.050D+00	9.12229D-01	9.11704D-01
2.100D+00	9.11603D-01	9.11024D-01
2.150D+00	9.10973D-01	9.10336D-01
2.200D+00	9.10339D-01	9.09639D-01
2.250D+00	9.09701D-01	9.08932D-01
2.300D+00	9.09058D-01	9.08216D-01
2.350D+00	9.08412D-01	9.07488D-01

Table III continued

2.400D+00	9.07760D-01	9.06749D-01
2.450D+00	9.07103D-01	9.05998D-01
2.500D+00	9.06442D-01	9.05233D-01
2.550D+00	9.05775D-01	9.04455D-01
2.600D+00	9.05103D-01	9.03662D-01
2.650D+00	9.04425D-01	9.02853D-01
2.700D+00	9.03741D-01	9.02027D-01
2.750D+00	9.03051D-01	9.01183D-01
2.800D+00	9.02355D-01	9.00319D-01
2.850D+00	9.01652D-01	8.99434D-01
2.900D+00	9.00942D-01	8.98527D-01
2.950D+00	9.00225D-01	8.97595D-01
3.000D+00	8.99501D-01	8.96636D-01
3.050D+00	8.98768D-01	8.95648D-01
3.100D+00	8.98028D-01	8.94630D-01
3.150D+00	8.97279D-01	8.93578D-01
3.200D+00	8.96521D-01	8.92490D-01
3.250D+00	8.95754D-01	8.91362D-01
3.300D+00	8.94977D-01	8.90191D-01
3.350D+00	8.94191D-01	8.88973D-01
3.400D+00	8.93393D-01	8.87703D-01
3.450D+00	8.92585D-01	8.86377D-01
3.500D+00	8.91765D-01	8.84987D-01
3.550D+00	8.90932D-01	8.83529D-01
3.600D+00	8.90086D-01	8.81993D-01
3.650D+00	8.89225D-01	8.80372D-01
3.700D+00	8.88348D-01	8.78655D-01
3.750D+00	8.87455D-01	8.76832D-01
3.800D+00	8.86542D-01	8.74888D-01
3.850D+00	8.85609D-01	8.72808D-01
3.900D+00	8.84651D-01	8.70574D-01
3.950D+00	8.83667D-01	8.68037D-01
4.000D+00	8.82651D-01	8.61939D-01
4.050D+00	8.81599D-01	8.55347D-01
4.100D+00	8.80505D-01	8.48534D-01
4.150D+00	8.79362D-01	8.41448D-01
4.200D+00	8.78161D-01	8.34017D-01
4.250D+00	8.76890D-01	8.26128D-01
4.300D+00	8.75537D-01	8.17850D-01
4.350D+00	8.74085D-01	8.09259D-01
4.400D+00	8.72512D-01	7.99953D-01
4.450D+00	8.70792D-01	7.89789D-01
4.500D+00	8.35980D-01	7.28442D-01
4.550D+00	8.11817D-01	6.54173D-01
4.600D+00	8.09375D-01	5.97628D-01
4.650D+00	8.06508D-01	5.43449D-01
4.700D+00	8.03050D-01	4.89260D-01
4.750D+00	7.98693D-01	4.29691D-01
4.800D+00	7.94673D-01	3.57946D-01
4.850D+00	7.92544D-01	3.37949D-01
4.900D+00	7.91926D-01	3.32408D-01
4.950D+00	7.91926D-01	3.32453D-01
5.000D+00	7.91926D-01	3.27938D-01

Table IV. Energy Spectrum for Monoenergetic Gamma Rays in a Spherical Shell of BGO. Configuration I, R_i=10cm, R_o=20cm

(Each gamma energy E is divided in ten equal bins, ΔSW is the difference of SW at the lower and upper end of the respective energy bin)

	ENERGY BIN									
E (MeV)	1	2	3	4	5	6	7	8	9	10
				ΔSW(MIN)						
0.5	0.03	0.10	0.25	0.44	0.64	0.87	1.30	0.77	0.04	95.57
1.0	1.23	0.35	0.48	0.79	1.30	2.06	3.14	5.26	4.15	81.25
2.0	5.11	0.84	0.82	0.90	1.23	2.33	3.53	8.80	15.19	61.25
3.0	6.61	0.82	0.81	0.86	1.01	1.33	2.86	5.53	22.31	57.85
4.0	6.99	0.70	0.71	0.75	0.85	1.06	1.51	4.29	21.44	61.70
5.0	6.95	0.58	0.60	0.64	0.71	0.86	1.16	2.30	13.35	72.84
6.0	6.72	0.48	0.50	0.54	0.60	0.71	0.94	1.51	6.82	81.17
7.0	6.40	0.40	0.42	0.46	0.51	0.60	0.78	1.21	5.28	83.94
8.0	6.04	0.34	0.36	0.39	0.43	0.51	0.65	0.99	3.70	86.59
9.0	5.68	0.29	0.31	0.33	0.37	0.44	0.56	0.83	2.70	88.49
10.0	5.32	0.25	0.26	0.29	0.32	0.38	0.48	0.70	1.71	90.29
				ΔSW(MAX)						
0.5	0.01	0.	0.	0.	0.	0.	0.	0.	0.	99.99
1.0	1.21	0.23	0.15	0.09	0.06	0.05	0.09	0.23	0.14	97.75
2.0	5.10	0.80	0.69	0.59	0.52	0.52	0.61	1.93	1.90	87.35
3.0	6.60	0.81	0.76	0.74	0.73	0.75	0.82	1.04	4.98	82.77
4.0	6.99	0.69	0.68	0.69	0.72	0.76	0.83	0.99	6.22	81.42
5.0	6.95	0.58	0.58	0.61	0.64	0.69	0.77	0.91	4.67	83.60
6.0	6.72	0.48	0.49	0.52	0.56	0.61	0.69	0.82	1.17	87.93
7.0	6.40	0.40	0.42	0.44	0.48	0.54	0.62	0.74	1.03	88.93
8.0	6.04	0.34	0.36	0.38	0.41	0.47	0.54	0.66	0.90	89.89
9.0	5.68	0.29	0.30	0.33	0.36	0.41	0.48	0.59	0.80	90.77
10.0	5.32	0.25	0.26	0.28	0.31	0.36	0.42	0.53	0.72	91.55

Table V. Energy Spectrum for Monoenergetic Gamma Rays in a Spherical Shell of BGO. Configuration II, R_i = 8cm, R_o = 18cm

(Each gamma energy E is divided in ten equal bins, ΔSW is the difference of SW at the lower and upper end of the respective energy bin)

	ENERGY BIN									
E (MeV)	1	2	3	4	5	6	7	8	9	10
				ΔSW(MIN)						
0.5	0.03	0.10	0.25	0.44	0.64	0.87	1.30	0.77	0.03	95.57
1.0	1.23	0.35	0.48	0.79	1.30	2.06	3.14	5.26	4.15	81.24
2.0	5.11	0.84	0.82	0.90	1.24	2.34	3.54	8.80	15.18	61.21
3.0	6.61	0.82	0.82	0.87	1.02	1.34	2.88	5.55	22.30	57.80
4.0	6.99	0.70	0.71	0.76	0.86	1.07	1.52	4.31	21.45	61.64
5.0	6.95	0.58	0.60	0.64	0.72	0.86	1.17	2.32	13.38	72.78
6.0	6.72	0.48	0.50	0.54	0.60	0.72	0.95	1.52	6.86	81.12
7.0	6.40	0.40	0.42	0.46	0.51	0.60	0.78	1.22	5.31	83.89
8.0	6.04	0.34	0.36	0.39	0.43	0.51	0.65	0.99	3.72	86.56
9.0	5.68	0.29	0.31	0.33	0.37	0.44	0.56	0.84	2.71	88.47
10.0	5.32	0.25	0.26	0.29	0.32	0.38	0.48	0.71	1.71	90.27
				ΔSW(MAX)						
0.5	0.01	0.	0.	0.	0.	0.	0.	0.	0.	99.99
1.0	1.21	0.23	0.15	0.09	0.06	0.05	0.09	0.23	0.14	97.74
2.0	5.10	0.80	0.69	0.59	0.53	0.53	0.62	1.93	1.90	87.31
3.0	6.60	0.81	0.77	0.74	0.74	0.76	0.82	1.05	4.99	82.72
4.0	6.99	0.69	0.69	0.70	0.72	0.77	0.84	1.00	6.22	81.38
5.0	6.95	0.58	0.59	0.61	0.64	0.70	0.78	0.92	4.67	83.56
6.0	6.72	0.48	0.49	0.52	0.56	0.62	0.70	0.83	1.18	87.90
7.0	6.40	0.40	0.42	0.45	0.48	0.54	0.62	0.75	1.04	88.90
8.0	6.04	0.34	0.36	0.38	0.42	0.47	0.55	0.67	0.91	89.87
9.0	5.68	0.29	0.30	0.33	0.36	0.41	0.48	0.60	0.81	90.75
10.0	5.32	0.25	0.26	0.28	0.31	0.36	0.43	0.53	0.72	91.53

Table VI. Energy Spectrum for Monoenergetic Gamma Rays in a Spherical Shell of BGO. Configuration III, R_i= 9cm, R_o=21cm

(Each gamma energy E is divided in ten equal bins, ΔSW is the difference of SW at the lower and upper end of the respective energy bin)

	ENERGY BIN									
E (MeV)	1	2	3	4	5	6	7	8	9	10
				ΔSW(MIN)						
0.5	0.02	0.10	0.25	0.44	0.64	0.87	1.30	0.77	0.03	95.58
1.0	0.51	0.22	0.40	0.75	1.30	2.07	3.15	5.22	4.12	82.24
2.0	2.80	0.54	0.57	0.70	1.05	1.97	3.25	8.88	15.40	64.84
3.0	3.83	0.56	0.56	0.62	0.79	1.16	2.40	4.79	22.86	62.43
4.0	4.10	0.48	0.49	0.54	0.64	0.86	1.35	3.54	21.53	66.48
5.0	4.07	0.40	0.42	0.45	0.53	0.67	0.99	2.03	12.36	78.08
6.0	3.91	0.33	0.35	0.38	0.43	0.54	0.77	1.37	5.51	86.41
7.0	3.69	0.28	0.29	0.32	0.36	0.44	0.61	1.05	4.21	88.74
8.0	3.45	0.23	0.25	0.27	0.31	0.37	0.50	0.83	3.00	90.81
9.0	3.20	0.20	0.21	0.23	0.26	0.31	0.42	0.68	2.24	92.25
10.0	2.96	0.17	0.18	0.20	0.22	0.27	0.35	0.56	1.52	93.58
				ΔSW(MAX)						
0.5	0.00	0.00	0.00	0.00	0.00	0.00	0.00	0.00	0.00	100.
1.0	0.49	0.10	0.06	0.03	0.02	0.02	0.03	0.08	0.06	99.10
2.0	2.80	0.50	0.42	0.34	0.29	0.28	0.36	1.64	1.22	92.16
3.0	3.82	0.54	0.50	0.47	0.46	0.47	0.52	0.69	4.62	87.89
4.0	4.10	0.47	0.46	0.47	0.48	0.50	0.55	0.67	6.10	86.20
5.0	4.07	0.40	0.40	0.41	0.44	0.47	0.52	0.61	4.52	88.16
6.0	3.91	0.33	0.34	0.36	0.38	0.42	0.47	0.55	0.81	92.43
7.0	3.69	0.28	0.29	0.30	0.33	0.37	0.42	0.50	0.70	93.13
8.0	3.45	0.23	0.24	0.26	0.28	0.32	0.37	0.44	0.60	93.80
9.0	3.20	0.19	0.21	0.22	0.24	0.28	0.32	0.40	0.53	94.41
10.0	2.96	0.16	0.18	0.19	0.21	0.24	0.29	0.35	0.47	94.95

Table VII. Energy Spectrum for Monoenergetic Gamma Rays in a Spherical Shell of BGO. Configuration IV, R_i = 8cm, R_o = 20cm

(Each gamma energy E is divided in ten equal bins, ΔSW is the difference of SW at the lower and upper end of the respective energy bin)

	ENERGY BIN									
E (MeV)	1	2	3	4	5	6	7	8	9	10
				ΔSW(MIN)						
0.5	0.02	0.10	0.25	0.44	0.64	0.87	1.30	0.77	0.03	95.58
1.0	0.51	0.22	0.40	0.76	1.30	2.07	3.15	5.22	4.12	82.24
2.0	2.80	0.54	0.57	0.70	1.06	1.97	3.25	8.88	15.39	64.83
3.0	3.83	0.56	0.56	0.63	0.80	1.16	2.41	4.80	22.86	62.41
4.0	4.10	0.48	0.49	0.54	0.64	0.86	1.35	3.54	21.53	66.46
5.0	4.07	0.40	0.42	0.45	0.53	0.67	0.99	2.04	12.37	78.06
6.0	3.91	0.33	0.35	0.38	0.44	0.54	0.77	1.37	5.52	86.39
7.0	3.69	0.28	0.29	0.32	0.36	0.45	0.61	1.05	4.22	88.72
8.0	3.45	0.23	0.25	0.27	0.31	0.37	0.50	0.83	3.00	90.80
9.0	3.20	0.20	0.21	0.23	0.26	0.31	0.42	0.68	2.24	92.25
10.0	2.96	0.17	0.18	0.20	0.22	0.27	0.35	0.56	1.52	93.57
				ΔSW(MAX)						
0.5	0.	0.	0.	0.	0.	0.	0.	0.	0.	100.
1.0	0.49	0.10	0.06	0.03	0.02	0.02	0.03	0.09	0.06	99.09
2.0	2.80	0.50	0.42	0.34	0.29	0.29	0.36	1.64	1.22	92.14
3.0	3.82	0.54	0.50	0.48	0.47	0.48	0.53	0.70	4.62	87.87
4.0	4.10	0.47	0.46	0.47	0.48	0.51	0.55	0.67	6.10	86.19
5.0	4.07	0.40	0.40	0.42	0.44	0.47	0.52	0.62	4.52	88.15
6.0	3.91	0.33	0.34	0.36	0.38	0.42	0.47	0.56	0.81	92.42
7.0	3.69	0.28	0.29	0.31	0.33	0.37	0.42	0.50	0.70	93.12
8.0	3.45	0.23	0.24	0.26	0.28	0.32	0.37	0.45	0.61	93.79
9.0	3.20	0.19	0.21	0.22	0.25	0.28	0.32	0.40	0.53	94.40
10.0	2.96	0.16	0.18	0.19	0.21	0.24	0.29	0.35	0.47	94.94

Table VIII. Energy Spectrum for Monoenergetic Gamma Rays in a Spherical Shell of BGO. Configuration V,R_i=10cm,R_o=18cm

(Each gamma energy E is divided in ten equal bins,ΔSW is the difference of SW at the lower and upper end of the respective energy bin)

	ENERGY BIN									
E (MeV)	1	2	3	4	5	6	7	8	9	10
				ΔSW(MIN)						
0.5	0.09	0.11	0.25	0.44	0.64	0.87	1.30	0.77	0.03	95.49
1.0	2.98	0.62	0.65	0.87	1.32	2.04	3.14	5.36	4.19	78.83
2.0	9.30	1.28	1.20	1.23	1.56	2.99	4.04	8.64	14.67	55.10
3.0	11.39	1.17	1.15	1.19	1.32	1.60	3.66	6.83	21.35	50.33
4.0	11.91	0.98	0.99	1.03	1.13	1.33	1.73	5.60	21.42	53.88
5.0	11.85	0.81	0.83	0.87	0.96	1.11	1.40	2.73	15.18	64.25
6.0	11.53	0.67	0.69	0.74	0.81	0.94	1.17	1.71	9.13	72.61
7.0	11.09	0.57	0.59	0.63	0.69	0.80	0.99	1.42	7.17	76.05
8.0	10.60	0.48	0.50	0.54	0.59	0.69	0.85	1.20	4.94	79.62
9.0	10.08	0.41	0.43	0.47	0.52	0.60	0.74	1.03	3.49	82.23
10.0	9.57	0.36	0.38	0.41	0.45	0.52	0.64	0.90	2.00	84.78
				ΔSW(MAX)						
0.5	0.08	0.01	0.	0.	0.	0.	0.	0.	0.	99.90
1.0	2.97	0.52	0.35	0.22	0.15	0.14	0.23	0.57	0.33	94.52
2.0	9.29	1.24	1.10	0.98	0.90	0.89	1.00	2.33	2.82	79.45
3.0	11.39	1.16	1.12	1.10	1.11	1.14	1.23	1.51	5.40	74.84
4.0	11.91	0.97	0.97	0.99	1.03	1.10	1.21	1.43	6.31	74.06
5.0	11.85	0.80	0.82	0.85	0.90	0.99	1.11	1.31	4.83	76.54
6.0	11.53	0.67	0.69	0.72	0.78	0.86	0.99	1.18	1.64	80.93
7.0	11.09	0.57	0.59	0.62	0.67	0.75	0.87	1.07	1.47	82.30
8.0	10.60	0.48	0.50	0.53	0.58	0.65	0.77	0.95	1.30	83.63
9.0	10.08	0.41	0.43	0.46	0.51	0.57	0.68	0.85	1.17	84.84
10.0	9.57	0.36	0.37	0.40	0.44	0.50	0.60	0.76	1.06	85.92

Table IX. Energy Spectrum for Monoenergetic Gamma Rays in a Spherical Shell of BGO. Configuration VI, R_i= 8cm, R_o=16cm

(Each gamma energy E is divided in ten equal bins, ΔSW is the difference of SW at the lower and upper end of the respective energy bin)

	ENERGY BIN									
E (MeV)	1	2	3	4	5	6	7	8	9	10
				ΔSW(MIN)						
0.5	0.09	0.11	0.25	0.44	0.64	0.87	1.30	0.77	0.03	95.49
1.0	2.98	0.63	0.66	0.87	1.32	2.04	3.14	5.37	4.18	78.81
2.0	9.30	1.28	1.21	1.24	1.57	3.02	4.07	8.65	14.65	55.02
3.0	11.40	1.17	1.16	1.20	1.33	1.61	3.69	6.88	21.35	50.22
4.0	11.91	0.98	0.99	1.04	1.14	1.34	1.74	5.65	21.45	53.76
5.0	11.85	0.81	0.83	0.88	0.96	1.11	1.41	2.75	15.27	64.13
6.0	11.53	0.67	0.70	0.74	0.81	0.94	1.18	1.71	9.21	72.50
7.0	11.09	0.57	0.59	0.63	0.69	0.80	1.00	1.43	7.23	75.97
8.0	10.60	0.48	0.50	0.54	0.60	0.69	0.85	1.20	4.98	79.56
9.0	10.08	0.41	0.43	0.47	0.52	0.60	0.74	1.04	3.52	82.19
10.0	9.57	0.36	0.38	0.41	0.45	0.52	0.65	0.90	2.01	84.75
				ΔSW(MAX)						
0.5	0.08	0.01	0.00	0.00	0.00	0.00	0.00	0.00	0.00	0.950
1.0	2.97	0.53	0.36	0.23	0.15	0.14	0.24	0.57	0.33	94.48
2.0	9.29	1.25	1.11	0.99	0.91	0.90	1.01	2.34	2.82	79.38
3.0	11.39	1.16	1.12	1.10	1.11	1.15	1.25	1.53	5.40	74.78
4.0	11.91	0.97	0.97	0.99	1.04	1.11	1.23	1.44	6.32	74.01
5.0	11.85	0.81	0.82	0.85	0.91	0.99	1.12	1.32	4.84	76.49
6.0	11.53	0.67	0.69	0.73	0.78	0.86	0.99	1.19	1.66	80.89
7.0	11.09	0.57	0.59	0.62	0.67	0.75	0.88	1.08	1.48	82.27
8.0	10.60	0.48	0.50	0.53	0.58	0.66	0.77	0.96	1.32	83.60
9.0	10.08	0.41	0.43	0.46	0.51	0.57	0.68	0.86	1.18	84.81
10.0	9.57	0.36	0.38	0.40	0.44	0.51	0.60	0.77	1.07	85.90

Table X. Energy Spectrum for Monoenergetic Gamma Rays in a Spherical Shell of BaF_2. Configuration I, R_i=10cm, R_o=22.5cm

(Each gamma energy E is divided in ten equal bins, ΔSW is the difference of SW at the lower and upper end of the respective energy bin)

	ENERGY BIN									
E (MeV)	1	2	3	4	5	6	7	8	9	10
				ΔSW(MIN)						
0.5	0.64	0.44	0.92	1.65	2.57	3.75	5.94	4.23	0.24	79.61
1.0	4.11	0.99	1.10	1.53	2.41	3.99	6.73	12.62	12.41	54.11
2.0	9.96	1.47	1.42	1.52	1.89	3.00	4.59	10.28	22.67	43.19
3.0	12.51	1.37	1.36	1.42	1.59	1.98	3.51	6.51	22.96	46.79
4.0	13.48	1.17	1.18	1.24	1.37	1.63	2.19	5.03	20.52	52.18
5.0	13.76	0.99	1.02	1.07	1.18	1.37	1.77	3.08	13.59	62.18
6.0	13.69	0.85	0.87	0.92	1.01	1.17	1.48	2.22	8.03	69.75
7.0	13.44	0.73	0.75	0.80	0.88	1.02	1.27	1.86	6.40	72.86
8.0	13.09	0.63	0.65	0.70	0.77	0.88	1.09	1.56	4.70	75.93
9.0	12.67	0.55	0.57	0.61	0.67	0.78	0.96	1.36	3.62	78.20
10.0	12.23	0.48	0.50	0.54	0.60	0.69	0.85	1.19	2.51	80.42
				ΔSW(MAX)						
0.5	0.60	0.12	0.05	0.02	0.01	0.03	0.07	0.05	0.	99.05
1.0	4.09	0.84	0.63	0.47	0.38	0.41	0.62	1.31	0.87	90.40
2.0	9.96	1.43	1.29	1.20	1.17	1.21	1.42	2.68	4.29	75.35
3.0	12.50	1.35	1.31	1.30	1.33	1.41	1.60	2.07	5.96	71.18
4.0	13.48	1.17	1.16	1.19	1.24	1.35	1.53	1.92	6.54	70.44
5.0	13.76	0.99	1.00	1.04	1.11	1.21	1.39	1.73	5.21	72.56
6.0	13.69	0.84	0.86	0.90	0.97	1.07	1.24	1.55	2.36	76.51
7.0	13.44	0.73	0.75	0.79	0.85	0.95	1.11	1.40	2.11	77.87
8.0	13.09	0.63	0.65	0.69	0.75	0.84	0.99	1.25	1.85	79.26
9.0	12.67	0.55	0.57	0.61	0.66	0.74	0.88	1.12	1.65	80.55
10.0	12.23	0.48	0.50	0.54	0.59	0.66	0.79	1.01	1.49	81.71

Table XI. Energy Spectrum for Monoenergetic Gamma Rays in a Spherical Shell of BaF_2. Configuration II, R_i=10cm, R_o=25cm

(Each gamma energy E is divided in ten equal bins, ΔSW is the difference of SW at the lower and upper end of the respective energy bin)

	ENERGY BIN									
E (MeV)	1	2	3	4	5	6	7	8	9	10
				ΔSW(MIN)						
0.5	0.25	0.37	0.90	1.66	2.59	3.77	5.95	4.23	0.24	80.05
1.0	2.15	0.65	0.87	1.40	2.39	4.04	6.82	12.74	12.62	56.31
2.0	6.26	1.07	1.06	1.20	1.62	2.69	4.46	10.69	23.78	47.17
3.0	8.23	1.05	1.05	1.12	1.32	1.75	3.15	6.14	24.30	51.89
4.0	9.01	0.92	0.93	0.99	1.12	1.39	2.00	4.52	21.35	57.76
5.0	9.24	0.79	0.81	0.86	0.96	1.15	1.56	2.85	13.30	68.49
6.0	9.20	0.67	0.69	0.74	0.82	0.97	1.28	2.07	7.19	76.35
7.0	9.00	0.58	0.60	0.64	0.71	0.84	1.08	1.68	5.64	79.23
8.0	8.71	0.50	0.52	0.56	0.62	0.72	0.92	1.38	4.15	81.92
9.0	8.38	0.43	0.45	0.49	0.54	0.63	0.80	1.19	3.25	83.83
10.0	8.03	0.38	0.40	0.43	0.48	0.56	0.70	1.02	2.33	85.69
				ΔSW(MAX)						
0.5	0.21	0.04	0.02	0.01	0.	0.01	0.02	0.01	0.	99.68
1.0	2.13	0.48	0.34	0.24	0.19	0.20	0.31	0.75	0.51	94.85
2.0	6.25	1.02	0.90	0.82	0.78	0.81	0.97	2.18	3.17	83.09
3.0	8.23	1.03	0.98	0.96	0.98	1.03	1.17	1.56	5.39	78.66
4.0	9.01	0.91	0.90	0.91	0.95	1.03	1.16	1.47	6.31	77.34
5.0	9.24	0.78	0.79	0.82	0.86	0.94	1.08	1.34	4.97	79.17
6.0	9.20	0.67	0.68	0.71	0.76	0.84	0.97	1.20	1.86	83.09
7.0	8.99	0.58	0.59	0.63	0.68	0.75	0.88	1.09	1.66	84.16
8.0	8.71	0.50	0.52	0.55	0.59	0.67	0.78	0.98	1.45	85.26
9.0	8.38	0.43	0.45	0.48	0.52	0.59	0.70	0.88	1.28	86.29
10.0	8.03	0.38	0.40	0.42	0.46	0.53	0.62	0.79	1.15	87.22

Table XII. Energy Spectrum for Monoenergetic Gamma Rays in a Spherical Shell of BaF_2. Configuration III, R_i=10cm, R_o=27.5cm

(Each gamma energy E is divided in ten equal bins, ΔSW is the difference of SW at the lower and upper end of the respective energy bin)

	ENERGY BIN									
E (MeV)	1	2	3	4	5	6	7	8	9	10
				ΔSW(MIN)						
0.5	0.12	0.35	0.89	1.66	2.59	3.78	5.95	4.23	0.24	80.20
1.0	1.13	0.45	0.74	1.34	2.39	4.09	6.88	12.74	12.67	57.56
2.0	3.92	0.77	0.80	0.98	1.44	2.50	4.39	10.95	24.43	49.83
3.0	5.42	0.79	0.79	0.88	1.10	1.57	2.90	5.91	25.20	55.44
4.0	6.03	0.70	0.72	0.77	0.91	1.20	1.85	4.17	21.97	61.68
5.0	6.21	0.61	0.62	0.67	0.77	0.96	1.39	2.68	13.16	72.93
6.0	6.17	0.52	0.54	0.58	0.66	0.80	1.11	1.94	6.65	81.03
7.0	6.02	0.45	0.47	0.50	0.56	0.68	0.92	1.53	5.13	83.74
8.0	5.80	0.38	0.40	0.43	0.49	0.58	0.76	1.23	3.78	86.14
9.0	5.54	0.33	0.35	0.38	0.42	0.50	0.66	1.04	2.99	87.77
10.0	5.28	0.29	0.31	0.33	0.37	0.44	0.57	0.87	2.19	89.36
				ΔSW(MAX)						
0.5	0.07	0.01	0.01	0.	0.	0.01	0.01	0.	0.	99.89
1.0	1.10	0.26	0.18	0.12	0.09	0.09	0.15	0.37	0.26	97.36
2.0	3.92	0.71	0.62	0.54	0.50	0.53	0.65	1.79	2.27	88.48
3.0	5.42	0.77	0.72	0.70	0.70	0.73	0.84	1.15	4.86	84.12
4.0	6.03	0.69	0.68	0.69	0.71	0.76	0.86	1.10	6.07	82.42
5.0	6.21	0.60	0.61	0.62	0.66	0.71	0.81	1.01	4.74	84.03
6.0	6.17	0.52	0.53	0.55	0.59	0.64	0.74	0.91	1.43	87.92
7.0	6.02	0.44	0.46	0.48	0.52	0.58	0.67	0.83	1.27	88.74
8.0	5.80	0.38	0.40	0.42	0.46	0.51	0.60	0.74	1.10	89.59
9.0	5.54	0.33	0.35	0.37	0.40	0.45	0.53	0.66	0.96	90.39
10.0	5.28	0.29	0.30	0.32	0.36	0.40	0.48	0.60	0.86	91.12

Table XIII. Energy Spectrum for Monoenergetic Gamma Rays in a Spherical Shell of BaF_2. Configuration IV, R_i=10cm, R_o=30cm

(Each gamma energy E is divided in ten equal bins, ΔSW is the difference of SW at the lower and upper end of the respective energy bin)

	ENERGY BIN									
E (MeV)	1	2	3	4	5	6	7	8	9	10
				ΔSW(MIN)						
0.5	0.07	0.34	0.89	1.66	2.60	3.78	5.95	4.23	0.24	80.25
1.0	0.60	0.33	0.67	1.31	2.40	4.12	6.92	12.75	12.70	58.21
2.0	2.46	0.55	0.61	0.83	1.32	2.37	4.33	11.11	24.82	51.60
3.0	3.57	0.58	0.60	0.69	0.93	1.44	2.74	5.76	25.80	57.89
4.0	4.03	0.53	0.54	0.60	0.74	1.05	1.73	3.94	22.41	64.42
5.0	4.17	0.46	0.47	0.52	0.61	0.81	1.25	2.55	13.10	76.04
6.0	4.15	0.39	0.41	0.45	0.52	0.66	0.98	1.84	6.29	84.32
7.0	4.03	0.34	0.35	0.39	0.44	0.55	0.78	1.42	4.80	86.91
8.0	3.86	0.29	0.31	0.33	0.38	0.46	0.64	1.10	3.53	89.10
9.0	3.67	0.25	0.26	0.29	0.33	0.40	0.54	0.92	2.81	90.52
10.0	3.46	0.22	0.23	0.25	0.29	0.34	0.46	0.75	2.09	91.90
				ΔSW(MAX)						
0.5	0.02	0.	0.01	0.	0.	0.	0.01	0.	0.	99.96
1.0	0.57	0.14	0.10	0.06	0.04	0.05	0.07	0.18	0.13	98.66
2.0	2.45	0.48	0.41	0.35	0.31	0.32	0.42	1.51	1.59	92.15
3.0	3.56	0.56	0.52	0.49	0.48	0.51	0.59	0.83	4.42	88.04
4.0	4.03	0.52	0.50	0.50	0.52	0.55	0.62	0.81	5.84	86.12
5.0	4.17	0.45	0.45	0.46	0.49	0.53	0.60	0.75	4.53	87.57
6.0	4.14	0.39	0.40	0.41	0.44	0.48	0.55	0.67	1.08	91.43
7.0	4.03	0.34	0.35	0.36	0.39	0.43	0.50	0.61	0.95	92.04
8.0	3.86	0.29	0.30	0.32	0.35	0.39	0.45	0.55	0.82	92.69
9.0	3.67	0.25	0.26	0.28	0.30	0.34	0.40	0.49	0.71	93.30
10.0	3.46	0.22	0.23	0.24	0.27	0.30	0.36	0.44	0.63	93.85

Table XIV. Important Parameters of the Calculations of Capture Cascades

Nucleus	Binding Energy (MeV)	Average Multiplicity of Capture Cascade	Number of Cascades Used in the Efficiency calculation	Covered Percentage of Total Capture Cross Section
^{241}Am	5.5	4.8	1000	75.0
^{197}Au	6.5	4.1	1000	80.2
^{56}Fe	7.6	3.0	300	96.2

Table XV. The Ten Capture Cascades with the Highest Partial Cross Section for Neutron Capture in ^{56}Fe, ^{197}Au and ^{241}Am (neutron energy 30keV)

^{56}Fe

Sigma (b)	1.Gamma	2.Gamma	3.Gamma	4.Gamma
		(MeV)		
0.00315	7.652	0.014		
0.00288	7.666			
0.00195	7.299	0.353	0.014	
0.00113	5.212	2.454		
0.00102	6.401	1.251	0.014	
0.00099	4.140	3.512	0.014	
0.00080	5.940	1.726		
0.00077	4.140	3.526		
0.00069	6.038	1.614	0.014	
0.00069	3.549	4.103	0.014	

Sigma total = 0.034 barn

^{197}Au

Sigma (b)	1.Gamma	2.Gamma	3.Gamma	4.Gamma
		(MeV)		
0.00734	2.960	3.582		
0.00656	2.220	4.322		
0.00642	6.542			
0.00607	6.487	0.055		
0.00584	2.960	3.527	0.055	
0.00578	3.700	2.842		
0.00535	2.220	4.267	0.055	
0.00501	2.960	3.321	0.261	
0.00492	6.281	0.261		
0.00473	2.960	3.346	0.236	

Sigma total = 0.87 barn

^{241}Am

Sigma (b)	1.Gamma	2.Gamma	3.Gamma	4.Gamma
		(MeV)		
0.02131	2.467	1.850	1.203	0.050
0.01896	1.850	2.467	1.203	0.050
0.01781	2.467	1.850	1.178	0.075
0.01731	2.467	1.850	1.154	0.099
0.01686	3.084	1.234	1.203	0.050
0.01588	1.850	2.467	1.178	0.075
0.01560	2.467	1.850	1.253	
0.01540	1.850	2.467	1.154	0.099
0.01415	3.084	1.234	1.178	0.075
0.01393	1.850	2.467	1.253	

Sigma total = 2.8 barn

Table XVI. Efficiency of a Spherical Shell of BGO for Neutron Capture Cascades Emitted in the ^{241}Am+n Reaction in Dependence of the Threshold Energy E. (all values are given in percent)

	Results obtained assuming SW(MIN) for monoenergetic gamma rays						Results obtained assuming SW(MAX) for monoenergetic gamma rays					
	Configuration						Configuration					
	I	II	III	IV	V	VI	I	II	III	IV	V	VI
	R_i/R_o(cm)						R_i/R_o(cm)					
E	10/20	8/18	9/21	8/20	10/18	8/16	10/20	8/18	9/21	8/20	10/18	8/16
0.5	99.95	99.95	99.98	99.98	99.87	99.87	99.96	99.96	99.99	99.99	99.88	99.88
1.0	99.89	99.89	99.96	99.96	99.68	99.68	99.91	99.91	99.97	99.97	99.72	99.72
1.5	99.48	99.48	99.75	99.75	98.82	98.82	99.54	99.54	99.78	99.78	98.93	98.93
2.0	98.70	98.70	99.33	99.33	97.30	97.30	98.85	98.85	99.41	99.41	97.57	97.57
2.5	97.68	97.68	98.76	98.76	95.37	93.36	98.29	98.29	99.12	99.12	96.41	96.40
3.0	95.46	95.46	97.47	97.46	91.51	91.50	96.77	96.77	98.26	98.26	93.64	93.63
3.5	91.68	91.66	95.14	95.13	85.36	85.33	93.60	93.59	96.38	96.38	88.37	88.35
4.0	86.23	86.21	91.44	91.43	77.22	77.17	88.97	88.96	93.63	93.62	80.92	80.89
4.5	77.51	77.46	84.03	84.00	66.44	66.34	84.64	84.62	91.22	91.20	73.55	73.48
5.0	50.03	49.98	55.56	55.53	40.88	40.76	78.97	78.91	86.74	86.70	66.31	66.19

Table XVII. Efficiency of a Spherical Shell of BGO for Neutron Capture Cascades Emitted in the ^{197}Au+n Reaction in Dependence of the Threshold Energy E. (all values are given in percent)

	Results obtained assuming SW(MIN) for monoenergetic gamma rays						Results obtained assuming SW(MAX) for monoenergetic gamma rays					
	Configuration						Configuration					
	I	II	III	IV	V	VI	I	II	III	IV	V	VI
	R_i/R_o (cm)						R_i/R_o (cm)					
E	10/20	8/18	9/21	8/20	10/18	8/16	10/20	8/18	9/21	8/20	10/18	8/16
0.5	99.81	99.81	99.89	99.64	99.64	99.64	99.82	99.82	99.90	99.90	99.66	99.66
1.0	98.87	98.87	99.40	99.40	97.76	97.76	98.88	98.88	99.41	99.41	97.79	97.78
1.5	98.54	98.54	99.22	99.22	97.10	97.10	98.64	98.64	99.28	99.28	97.28	97.27
2.0	97.73	97.73	98.77	98.77	95.60	95.59	97.94	97.94	98.89	98.89	95.95	95.95
2.5	96.49	96.49	98.05	98.05	93.44	93.43	96.90	96.90	98.30	98.30	94.13	94.12
3.0	94.44	94.44	96.82	96.82	90.04	90.03	94.95	94.94	97.12	97.13	90.88	90.88
3.5	92.26	92.26	95.48	95.48	86.55	86.53	93.28	93.27	96.12	96.12	88.17	88.15
4.0	88.97	88.96	93.37	93.36	81.54	81.52	90.18	90.17	94.18	94.18	83.37	83.37
4.5	85.42	85.39	90.95	90.94	76.42	76.42	86.71	86.69	92.01	92.01	78.10	78.08
5.0	81.27	81.23	87.70	87.68	70.99	70.92	83.87	83.84	90.26	90.24	73.74	73.71
5.5	73.31	73.25	80.36	80.33	62.19	62.08	81.47	81.42	88.73	88.69	70.23	70.16
6.0	44.68	44.62	50.06	50.04	36.34	36.22	73.75	73.68	81.72	81.68	61.85	61.76

Table XVIII. Efficiency of a Spherical Shell of BGO for Neutron Capture Cascades Emitted in the $^{56}Fe+n$ Reaction in Dependence of the Threshold Energy E. (all values are given in percent)

	Results obtained assuming SW(MIN) for monoenergetic gamma rays						Results obtained assuming SW(MAX) for monoenergetic gamma rays					
	Configuration						Configuration					
	I	II	III	IV	V	VI	I	II	III	IV	V	VI
	R_i/R_o(cm)						R_i/R_o(cm)					
E	10/20	8/18	9/21	8/20	10/18	8/16	10/20	8/18	9/21	8/20	10/18	8/16
0.5	98.71	98.71	99.29	99.29	97.57	97.57	98.71	98.71	99.29	99.29	97.58	97.58
1.0	97.91	97.91	98.86	98.86	96.04	96.04	97.94	97.94	98.88	98.88	96.08	96.08
1.5	97.48	97.48	98.62	98.62	95.23	95.23	97.59	97.59	98.68	98.68	95.41	95.41
2.0	96.54	96.54	98.07	98.07	93.61	93.61	96.68	96.68	98.16	98.16	93.85	93.85
2.5	95.69	95.68	97.57	97.57	92.17	92.17	95.98	95.98	97.75	97.75	92.67	92.66
3.0	94.59	94.59	96.90	96.90	90.40	90.39	94.92	94.92	97.11	97.11	90.95	90.94
3.5	93.43	93.43	96.18	96.18	88.57	88.56	93.92	93.92	96.49	96.49	89.37	89.36
4.0	91.81	91.80	95.15	95.15	86.08	86.06	92.32	92.31	95.48	95.48	86.88	86.87
4.5	89.84	89.83	93.86	93.86	83.15	83.14	90.36	90.35	94.23	94.23	83.93	83.92
5.0	87.97	87.96	92.61	92.60	80.44	80.41	88.62	88.61	93.11	93.11	81.33	81.31
5.5	85.90	85.88	91.15	91.14	77.52	77.49	86.74	86.72	91.91	91.91	78.51	78.50
6.0	83.16	83.13	88.96	88.95	74.04	73.99	84.79	84.76	90.65	90.64	75.67	75.64
6.5	78.84	78.79	85.10	85.08	69.07	68.99	83.19	83.15	89.61	89.58	73.35	73.30
7.0	60.81	60.74	66.75	66.72	51.55	51.43	78.00	77.94	84.80	84.77	67.72	67.72

Table XIX. Efficiency of a Spherical Shell of BaF_2 for Neutron Capture Cascades Emitted in the $^{241}Am+n$ Reaction in Dependence of the Threshold Energy E (all values are given in percent).

	Results obtained assuming SW(MIN) for monoenergetic gamma rays				Results obtained assuming SW(MAX) for monoenergetic gamma rays			
	Configuration				Configuration			
	I	II	III	IV	I	II	III	IV
	R_i/R_o (cm)				R_i/R_o (cm)			
E	10/22.5	10/25	10/27.5	10/30	10/22.5	10/25	10/27.5	10/30
0.5	99.82	99.92	99.96	99.98	99.84	99.93	99.97	99.99
1.0	99.54	99.79	99.90	99.94	99.63	99.84	99.93	99.97
1.5	98.42	99.17	99.53	99.72	98.67	99.32	99.63	99.79
2.0	96.46	98.01	98.82	99.27	97.05	98.38	99.06	99.43
2.5	93.49	96.15	97.62	98.49	95.54	97.55	98.58	99.14
3.0	88.40	92.75	95.36	96.97	92.22	95.51	97.29	98.31
3.5	81.13	87.60	91.72	94.38	86.30	91.52	94.62	96.54
4.0	71.34	79.95	85.67	89.44	78.11	85.77	90.72	93.96
4.5	56.71	65.98	72.28	76.46	69.12	79.58	86.68	91.40
5.0	26.27	31.53	35.20	37.66	59.60	72.00	80.76	86.72

Table XX. Efficiency of a Spherical Shell of BaF_2 for Neutron Capture Cascades Emitted in the $^{197}Au+n$ Reaction in Dependence of the Threshold Energy E (all values are given in percent).

	Results obtained assuming SW(MIN) for monoenergetic gamma rays				Results obtained assuming SW(MAX) for monoenergetic gamma rays			
	Configuration				Configuration			
	I	II	III	IV	I	II	III	IV
	R_i/R_o (cm)				R_i/R_o (cm)			
E	10/22.5	10/25	10/27.5	10/30	10/22.5	10/25	10/27.5	10/30
0.5	99.49	99.69	99.81	99.87	99.57	99.74	99.84	99.90
1.0	97.25	98.37	99.00	99.36	97.31	98.42	99.03	99.39
1.5	96.28	97.80	98.64	99.14	96.65	98.04	98.81	99.25
2.0	94.47	96.65	97.90	98.65	95.06	97.06	98.19	98.85
2.5	91.87	94.92	96.74	97.87	92.92	95.68	97.29	98.26
3.0	87.99	92.24	94.90	96.62	89.16	93.11	95.54	97.07
3.5	83.78	89.23	92.79	95.14	86.04	90.95	94.06	96.07
4.0	78.32	85.18	89.85	93.02	80.72	87.09	91.32	94.16
4.5	72.69	80.79	86.47	90.40	75.05	82.89	88.32	92.08
5.0	66.31	75.27	81.67	86.15	70.10	79.24	85.75	90.32
5.5	56.24	65.07	71.45	75.94	65.65	75.84	83.28	88.59
6.0	29.31	34.43	38.17	40.82	55.81	66.85	75.28	81.48

Table XXI. Efficiency of a Spherical Shell of BaF_2 for Neutron Capture Cascades Emitted in the $^{56}Fe+n$ Reaction in Dependence of the Threshold Energy E (all values are given in percent).

	Results obtained assuming SW(MIN) for monoenergetic gamma rays				Results obtained assuming SW(MAX) for monoenergetic gamma rays			
	Configuration				Configuration			
	I	II	III	IV	I	II	III	IV
		R_i/R_o (cm)				R_i/R_o (cm)		
E	10/22.5	10/25	10/27.5	10/30	10/22.5	10/25	10/27.5	10/30
0.5	96.96	98.10	98.79	99.21	97.00	98.13	98.80	99.22
1.0	95.02	96.91	98.04	98.74	95.14	96.99	98.09	98.77
1.5	93.89	96.18	97.57	98.42	94.27	96.46	97.76	98.55
2.0	92.04	94.94	96.72	97.85	92.39	95.19	96.91	97.99
2.5	90.27	93.72	95.89	97.29	90.95	94.23	96.26	97.55
3.0	88.22	92.26	94.87	96.58	88.92	92.80	95.27	96.86
3.5	86.07	90.71	93.77	95.79	87.06	91.47	94.33	96.21
4.0	83.27	88.65	92.28	94.74	84.25	89.42	92.86	95.18
4.5	80.02	86.19	90.46	93.40	80.96	86.96	91.08	93.91
5.0	76.99	83.85	88.69	92.06	78.07	84.79	89.50	92.78
5.5	73.75	81.27	86.66	90.46	74.99	82.48	87.82	91.59
6.0	69.70	77.75	83.59	87.75	71.72	79.97	85.97	90.28
6.5	64.29	72.51	78.51	82.79	68.84	77.74	84.32	89.09
7.0	47.03	53.71	58.58	62.05	62.46	71.84	78.95	84.21

Table XXII. Difference in Efficiency ε(Sample)-ε(Reference Sample) as Expected in a Relative Measuerment of Capture Cross Section using a BGO Detector and a Gold Standard in Dependence of the Threshold Energy E (all values are given in percent).

	Results obtained assuming SW(MIN) for monoenergetic gamma rays						Results obtained assuming SW(MAX) for monoenergetic gamma rays					
	Configuration						Configuration					
	I	II	III	IV	V	VI	I	II	III	IV	V	VI
	R_i/R_o(cm)						R_i/R_o(cm)					
E	10/20	8/18	9/21	8/20	10/18	8/16	10/20	8/18	9/21	8/20	10/18	8/16
	$\sigma_\gamma(^{241}Am)/\sigma_\gamma(^{197}Au)$											
2.0	0.97	0.97	0.56	0.56	1.70	1.71	0.91	0.91	0.52	0.52	1.62	1.62
2.5	1.19	1.19	0.71	0.71	1.93	1.93	1.39	1.39	0.82	0.82	2.28	2.28
3.0	1.02	1.02	0.65	0.64	1.47	1.47	1.82	1.83	1.13	1.13	2.76	2.75
3.5	-0.58	-0.60	-0.34	-0.35	-1.19	-1.20	0.32	0.32	0.26	0.26	0.20	0.20
	$\sigma_\gamma(^{56}Fe)/\sigma_\gamma(^{197}Au)$											
2.0	-1.19	-1.19	-0.70	-0.70	-1.99	-1.99	-1.26	-1.26	-0.73	-0.73	-2.10	-2.10
2.5	-0.80	-0.81	-0.48	-0.48	-1.27	-1.26	-0.92	-0.92	-0.55	-0.55	-1.46	-1.46
3.0	0.15	0.15	0.08	0.08	0.36	0.36	-0.03	-0.02	-0.02	-0.02	0.07	0.06
3.5	1.17	1.17	0.70	0.70	2.02	2.03	0.64	0.65	0.37	0.37	1.20	1.21

Table XXIII. Difference in Efficiency ε(Sample)-ε(Reference Sample) as Expected in a Relative Measuerment of Capture Cross Section using a BaF_2 Detector and a Gold Standard in Dependence of the Threshold Energy E (all values are given in percent).

	Results obtained assuming SW(MIN) for monoenergetic gamma rays				Results obtained assuming SW(MAX) for monoenergetic gamma rays			
	Configuration				Configuration			
	I	II	III	IV	I	II	III	IV
	R_i/R_o (cm)				R_i/R_o (cm)			
E	10/22.5	10/25	10/27.5	10/30	10/22.5	10/25	10/27.5	10/30
	$\sigma_\gamma(^{241}Am)/\sigma_\gamma(^{197}Au)$							
2.0	1.99	1.36	0.92	0.62	1.99	1.32	0.87	0.58
2.5	1.62	1.23	0.88	0.62	2.62	1.87	1.29	0.88
3.0	0.41	0.51	0.46	0.35	3.06	2.40	1.75	1.24
3.5	-2.65	-1.63	-1.07	-0.76	0.26	0.57	0.56	0.47
	$\sigma_\gamma(^{56}Fe)/\sigma_\gamma(^{197}Au)$							
2.0	-2.43	-1.71	-1.18	-0.80	-2.67	-1.87	-1.28	-0.86
2.5	-1.60	-1.20	-0.85	-0.58	-1.97	-1.45	-1.03	-0.71
3.0	0.23	0.02	-0.03	-0.04	-0.24	-0.31	-0.27	-0.21
3.5	2.29	1.48	0.98	0.65	1.02	0.52	0.27	0.14

FIGURE CAPTIONS

Fig. 1 Calculated detection probability p for monoenergetic gamma rays with energy E_γ in a spherical shell of BGO (R_i = 10 cm, R_o = 20 cm). Each gamma energy E_γ is divided artificially into 10 bins to simulate an energy resolution of 10 %.

Fig. 2 Capture gamma ray spectra for neutron capture in ^{241}Am, ^{197}Au and ^{56}Fe as calculated according to the statistical model.

Fig. 3 Calculated pulse height spectrum of a spherical shell of BGO (R_i = 10 cm, R_o = 20 cm) for neutron capture in ^{56}Fe, ^{197}Au and ^{241}Am.

Fig. 4 Gamma-ray background measured with a cylindrical BGO detector (10 cm diameter, 10 cm thickness).

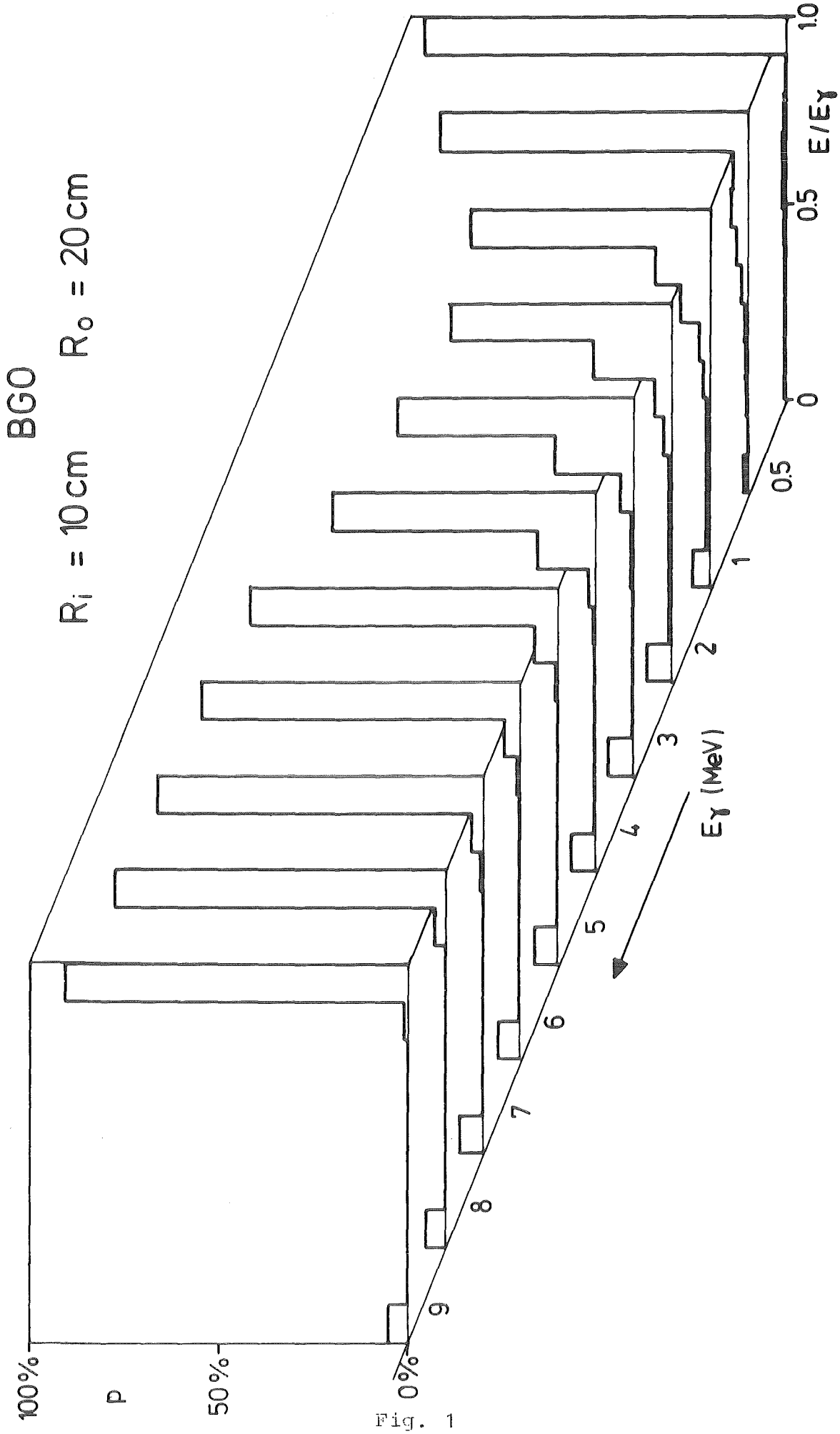

Fig. 1

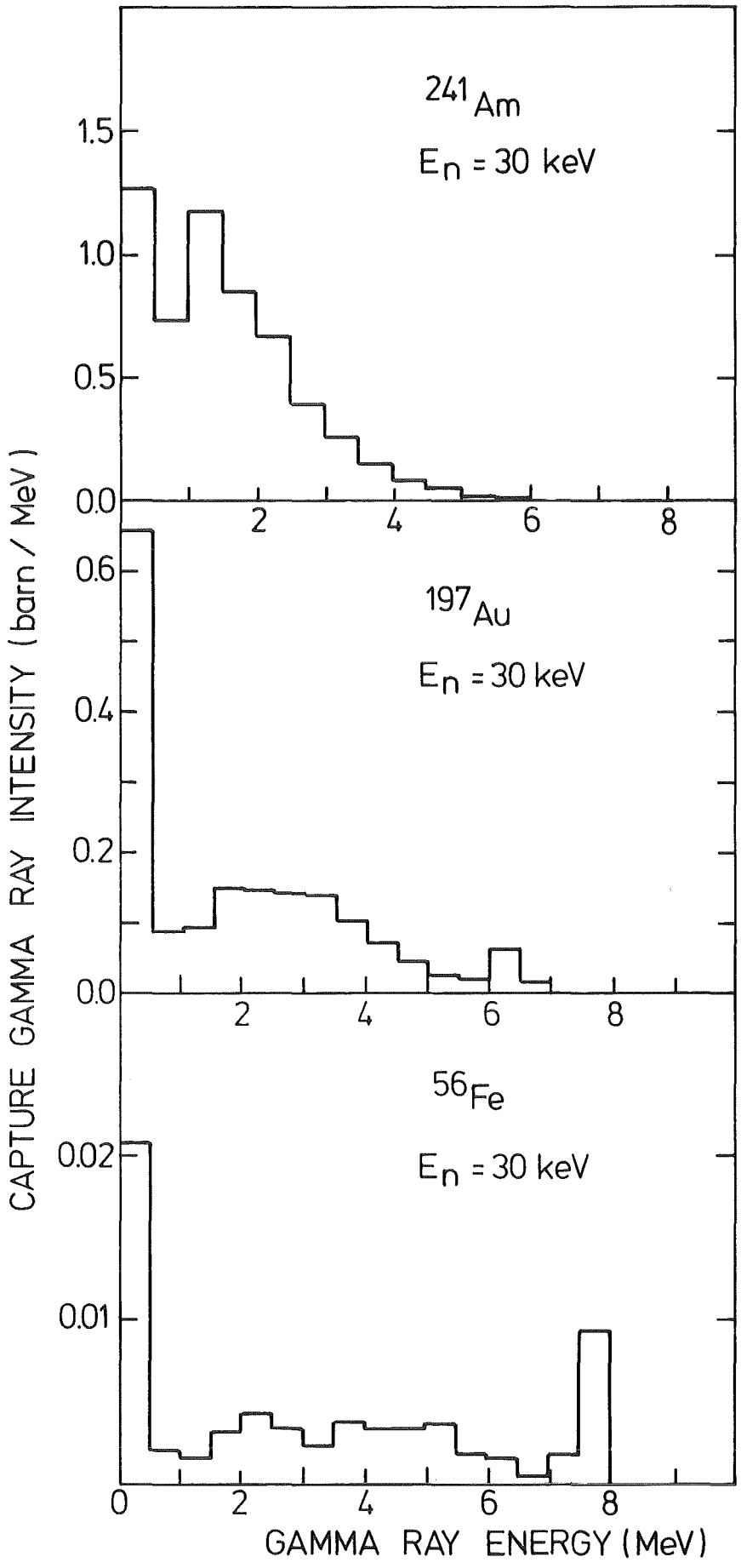
241Am
En = 30 keV
197Au
En = 30 keV
56Fe
En = 30 keV
CAPTURE GAMMA RAY INTENSITY (barn / MeV)
GAMMA RAY ENERGY (MeV)
1.5
1.0
0.5
0.0
0.6
0.4
0.2
0.0
0.02
0.01
0
2
4
6
8

Fig. 2

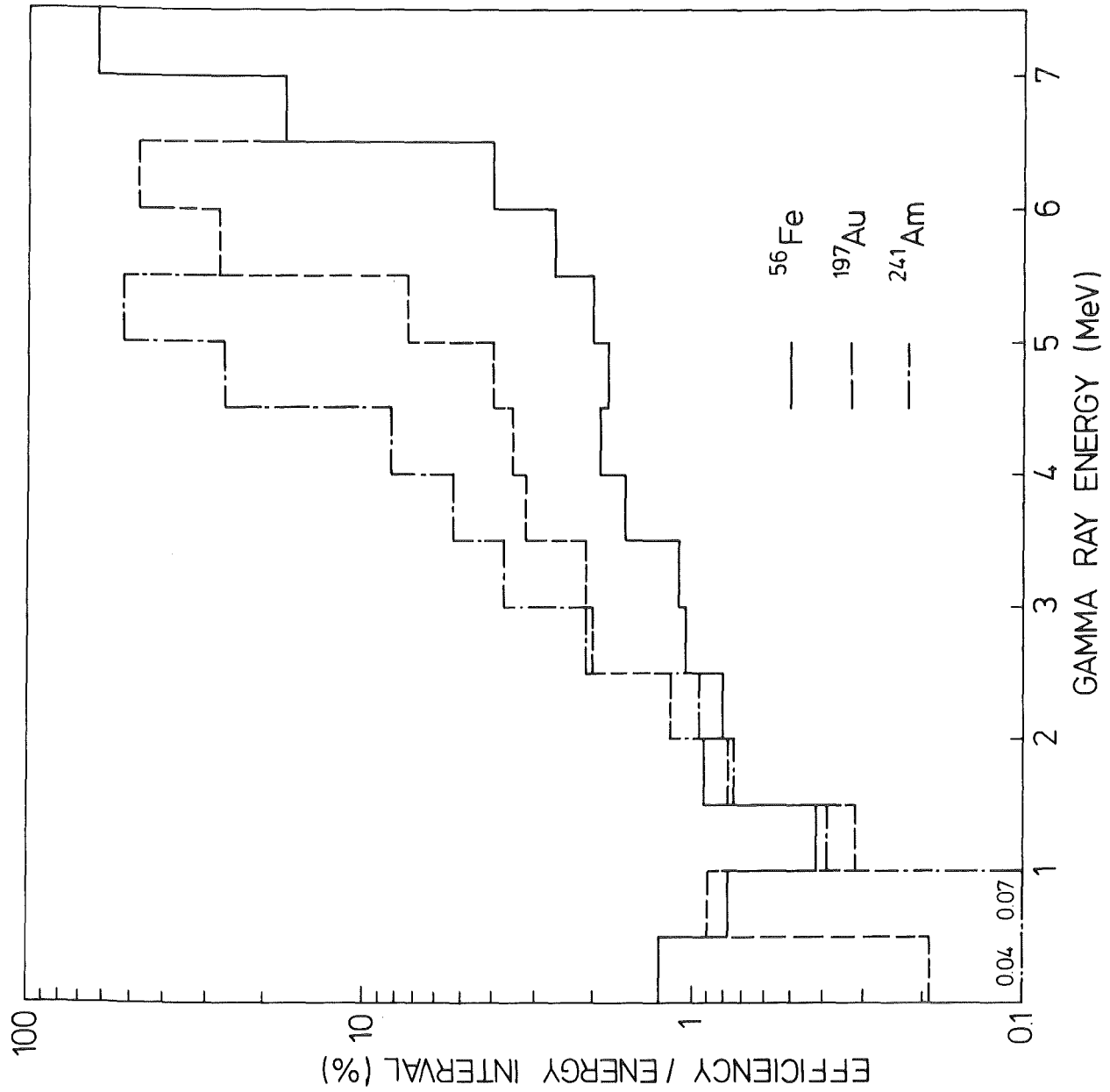
EFFICIENCY / ENERGY INTERVAL (%)
100
10
1
0.1
0.04
0.07
1
2
3
4
5
6
7
GAMMA RAY ENERGY (MeV)
56Fe
197Au
241Am

Fig. 3

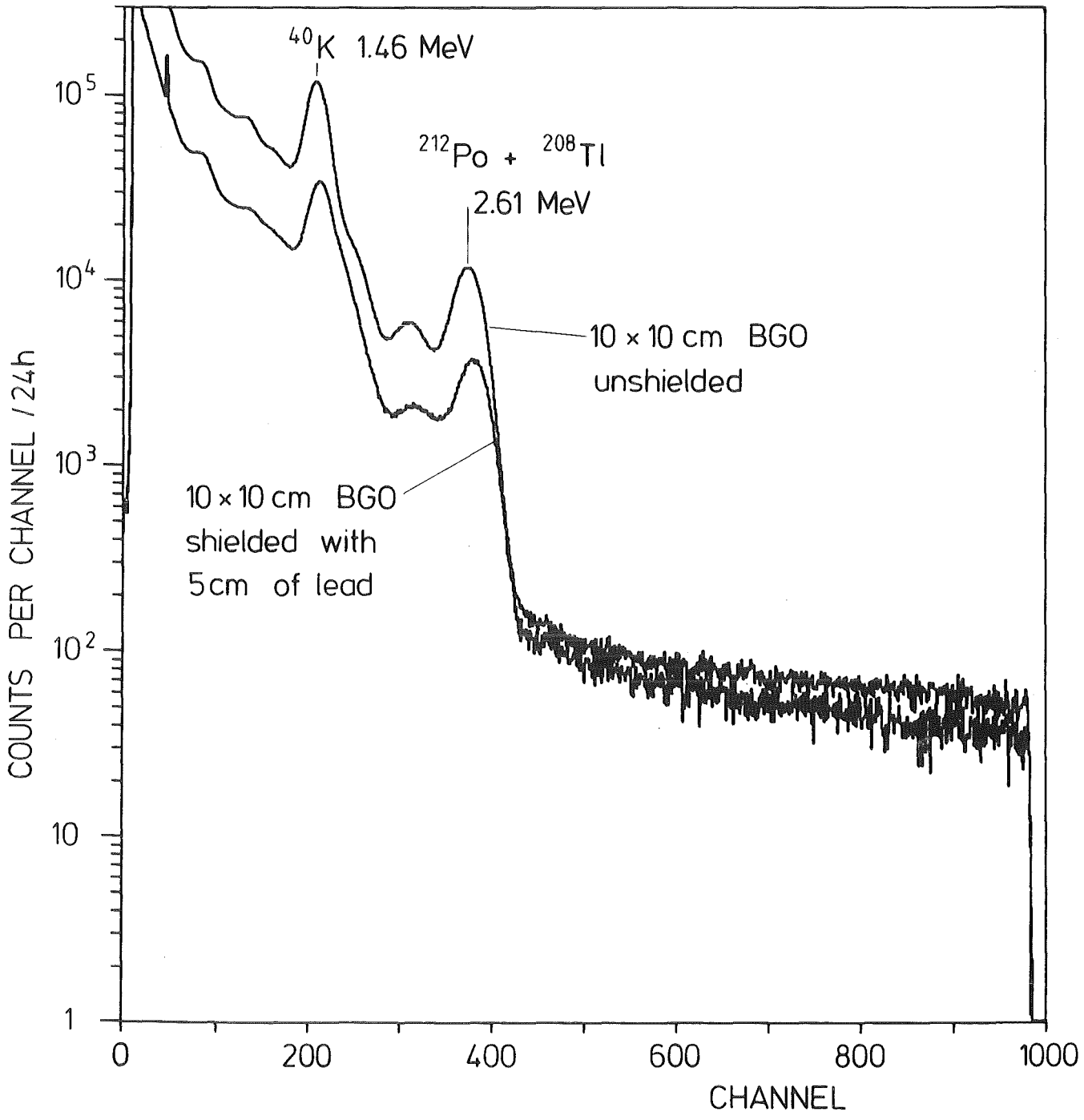
^{40}K 1.46 MeV
^{212}Po + ^{208}Tl
2.61 MeV
10 × 10 cm BGO
unshielded
10 × 10 cm BGO
shielded with
5 cm of lead
COUNTS PER CHANNEL / 24h
10^5
10^4
10^3
10^2
10
1
0
200
400
600
800
1000
CHANNEL

Fig. 4